
A Uniform Confidence Phenomenon in Deep Learning and its Implications for Calibration

Muthu Chidambaram

Department of Computer Science
Duke University
muthu@cs.duke.edu

Rong Ge

Department of Computer Science
Duke University
rongge@cs.duke.edu

Abstract

Despite the impressive generalization capabilities of deep neural networks, they have been repeatedly shown to poorly estimate their predictive uncertainty - in other words, they are frequently overconfident when they are wrong. Fixing this issue is known as model calibration, and has consequently received much attention in the form of modified training schemes and post-training calibration procedures. In this work, we present a significant hurdle to the calibration of modern models: deep neural networks have large neighborhoods of almost certain confidence around their training points. We demonstrate in our experiments that this phenomenon consistently arises (in the context of image classification) across many model and dataset pairs. Furthermore, we prove that when this phenomenon holds, for a large class of data distributions with overlaps between classes, it is not possible to obtain a model that is asymptotically better than random (with respect to calibration) even *after* applying the standard post-training calibration technique of temperature scaling. On the other hand, we also prove that it is possible to circumvent this defect by changing the training process to use a modified loss based on the Mixup data augmentation technique.

1 Introduction

The past decade has seen a rapid increase in the prevalence of deep learning models across a variety of applications, in large part due to their impressive predictive accuracy on unseen test data. However, as these models begin to be applied to critical applications such as predicting credit risk (Clements et al., 2020), diagnosing medical conditions (Esteva et al., 2017, 2021; Elmarakeby et al., 2021), and autonomous driving (Bojarski et al., 2016; Grigorescu et al., 2020), it is crucial that the models are not only accurate but also predict with appropriate levels of uncertainty.

In the context of classification, a model with appropriate uncertainty would be correct with a probability that is similar to its predicted confidence – for example, among samples on which the model predicts a class with 90% confidence, around 90% of them should indeed be the predicted class (a more formal definition is provided in Equation (3.1)).

As a concrete (but highly simplified) example, consider the case of applying a deep learning model for predicting whether a patient has a life-threatening illness (Jiang et al., 2012). In this situation, suppose our model classifies the patient as not having the illness but does so with high confidence. A physician using this model for their assessments may then incorrectly diagnose the patient (with potentially grave consequences). On the other hand, if the model had lower confidence in this incorrect prediction, a physician may be more likely to do further assessments.

Obtaining such models with good predictive uncertainty is the problem of *model calibration*, and has seen a flurry of recent work in the context of training deep learning models (Guo et al., 2017; Thulasidasan et al., 2019; Ovadia et al., 2019; Wen et al., 2020; Minderer et al., 2021). Without

these calibration techniques, it is commonly observed that large neural network models are often over-confident (Guo et al., 2017) – they can make incorrect predictions with very high confidence.

In this paper, we investigate what properties of trained neural networks lead to such overconfidence in practice, and whether these properties have further implications for how we should do model calibration. Our approach centers on analyzing model confidence in regions of the input space beyond just the training and test data. Such an analysis can allow us to predict model calibration performance for different training/test data distributions, and then consequently determine if there exist plausible distributions for which we cannot hope to be calibrated for.

This idea of attempting to understand the confidence of neural networks outside of the training and test data is not new; a recent line of work (Hein et al., 2019; Meinke & Hein, 2020; Kristiadi et al., 2020) has shown empirically and theoretically that certain classes of ReLU networks can have high confidence predictions far away from the data that they were trained on. To the best of our knowledge, however, prior work has not precisely characterized (empirically or theoretically) the nature of these high confidence regions and their impacts on calibration. In this work, we attempt to make progress on this problem by answering the following questions:

1. How does the confidence of trained neural networks change as we move away from the training and test data?
2. Does the confidence behavior of neural networks imply settings for which we cannot calibrate them using post-training calibration methods?

1.1 Main Contributions

Our main empirical finding can be summarized as:

Deep neural networks have large regions of almost certain confidence around their training data points, across a wide variety of architectures and data, so long as they are trained to zero training error.

It is not surprising that neural networks trained to achieve zero training error have softmax outputs that are effectively point masses at their training data points, as this is optimal for the empirical cross-entropy. What is surprising about our results is that these softmax outputs remain almost constant in relatively large neighborhoods around *all* of the training data points.

We empirically establish this phenomenon for various image classification models ranging from popular baselines to current state-of-the-art in Section 2. Our results are consistent across multiple classification benchmarks, and continue to hold even if the true labels of the data are replaced with random labels. The ramifications are significant - for data distributions in which the supports of different classes overlap, it may not be possible to calibrate modern models using standard techniques.

We formalize this idea into a theoretical framework in Section 3, and prove in Section 4 that for a wide class of data distributions, models following the aforementioned phenomenon are asymptotically no better than random classifiers in terms of calibration even **after** we apply post-training calibration techniques. On the other hand, we also prove that by using a generalization of Mixup training (Zhang et al., 2017b), we can achieve reasonably good calibration. The key takeaway from our theory is that *post-training calibration can fail to fix problems that are fixable by modifying the loss function.*

1.2 Related Work

Calibration in deep learning. The calibration of deep learning models has received significant attention in recent years, largely stemming from the work of Guo et al. (2017) which empirically showed that modern, overparameterized models can have poor predictive uncertainty. Follow-up works (Thulasidasan et al., 2019; Wen et al., 2021) have supported these findings, although the recent work of Minderer et al. (2021) showed that current state-of-the-art architectures can be better calibrated than the previous generation of models.

From a theoretical standpoint, work on calibration in deep learning is still nascent. As mentioned previously, the works of Hein et al. (2019) and Meinke & Hein (2020) showed that ReLU networks can have high confidence predictions away from their training data, but this does not by itself imply

poor calibration. In this work, we show that when models exhibit a more general high confidence phenomenon, they will be provably poorly calibrated with respect to a large class of distributions.

Methods for improving calibration. Many different methods have been proposed for improving calibration, including: logit rescaling (Guo et al., 2017), data augmentation (Thulasidasan et al., 2019; Müller et al., 2020), ensembling (Lakshminarayanan et al., 2017; Wen et al., 2020), and modified loss functions (Kumar et al., 2018; Wang et al., 2021). The logit rescaling methods, namely temperature scaling and its variants (Kull et al., 2019; Ding et al., 2020), constitute perhaps the most applied calibration techniques, since they can be used on any trained model with the introduction of only a few extra parameters (see Section 3.1). However, we show in this work that this kind of post-training calibration can be insufficient for some data distributions, which can in fact require data augmentation/modified loss functions to achieve good calibration. We focus particularly on Mixup (Zhang et al., 2017b) data augmentation, whose theoretical benefits for calibration were recently studied by Zhang et al. (2021) in the context of linear models and Gaussian data. Our results provide a complementary perspective to this prior work, as we address a much broader class of models and a different class of data distributions.

2 A Uniform Confidence Phenomenon

In this section we consider experimentally how the confidence of models change as we move away from training points. Given a classification training dataset \mathcal{X} , we first downsample \mathcal{X} to consist of 5000 points (approximately 10% of the original size of the datasets we consider) due to computational constraints (detailed below). Then, for every point $(x_i, y_i) \in \mathcal{X}$, we sample points uniformly from the surface of spheres (neighborhoods) centered around x_i with varying radii and compute the mean probability with which a trained model predicts the class y_i over these sampled points. Crucially, *the radii for the neighborhoods considered at each x_i vary with x_i* . This is because different points may have very different distances to the decision boundary, so it does not make sense to compute model predictions at fixed distances from each data point.

Instead, we define what we refer to as the **Other-Class Nearest Neighbor (OCNN)** distance, which for a point (x_i, y_i) is the minimum distance from x_i to another point x_j such that the label $y_j \neq y_i$. We sample batches of 500 points at different fixed proportions of the OCNN distance away from each x_i , and then take the mean of the predicted probability for the class y_i over these batches. We then report the mean and variance of original class (i.e. y_i) probabilities for each fixed proportion of the OCNN distance over the entire dataset. A visualization of this procedure is provided in Figure 1.

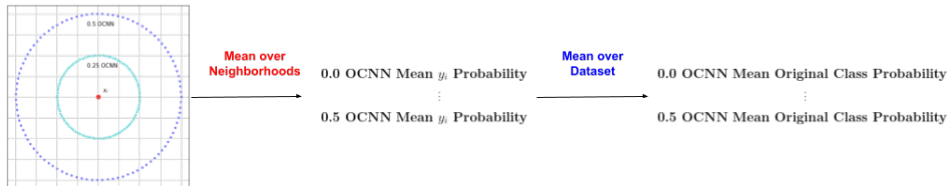


Figure 1: Visualization of our experimental setup.

Note that because our procedure requires computing nearest neighbor distances and sampling points conditional on these distances, it is not easy to vectorize and its computational cost scales quadratically in the dataset size (when implemented naively). While more efficient approaches to this computation exist, we have opted for downsampling the data due to its simplicity and easy reproducibility. Based on the consistency of our main experimental results, as well as the larger-scale explorations in Appendix B.4, we anticipate no significant changes to our findings as data size is scaled.

Findings. Our main evaluation results are shown in Figure 2, with all model/dataset details described in Section 2.1. We consider ten neighborhoods around each training point, corresponding to equally spaced OCNN distance proportions from 0 to 0.5 (with 0 indicating just the original point itself). We observe that the mean original class softmax prediction for **all models, over all datasets** remains almost **constant at 1** for a non-trivial radius around each training point. Additionally, we find that this radius of confidence (as a proportion of the OCNN distance) appears to be relatively consistent across models and datasets (around 0.2 to 0.3).

To get a sense of how surprising this is, we point out that it is known in the adversarial attack literature that moving roughly 0.1 (Euclidean distance) away from a data point is enough to flip the prediction of state-of-the-art deep learning models from the correct class to another class on CIFAR (Carlini & Wagner, 2017). On the other hand, the *minimum* OCNN distance over all of our datasets was on the order of 10. We interpret this to mean that even though adversarial directions can exist, on average it is possible to move a significant distance from a data point without affecting model predictions at all.

The lack of variance in Figure 2 up to 0.2-0.3 OCNN distance implies that this phenomenon holds at virtually every training data point, and hence we refer to it as **uniform confidence**. The main concern with a model exhibiting uniform confidence behavior is that any test data point from a class y that falls in a confidence neighborhood of a training data point from a class $s \neq y$ will not only be classified incorrectly, but classified incorrectly with very high confidence.

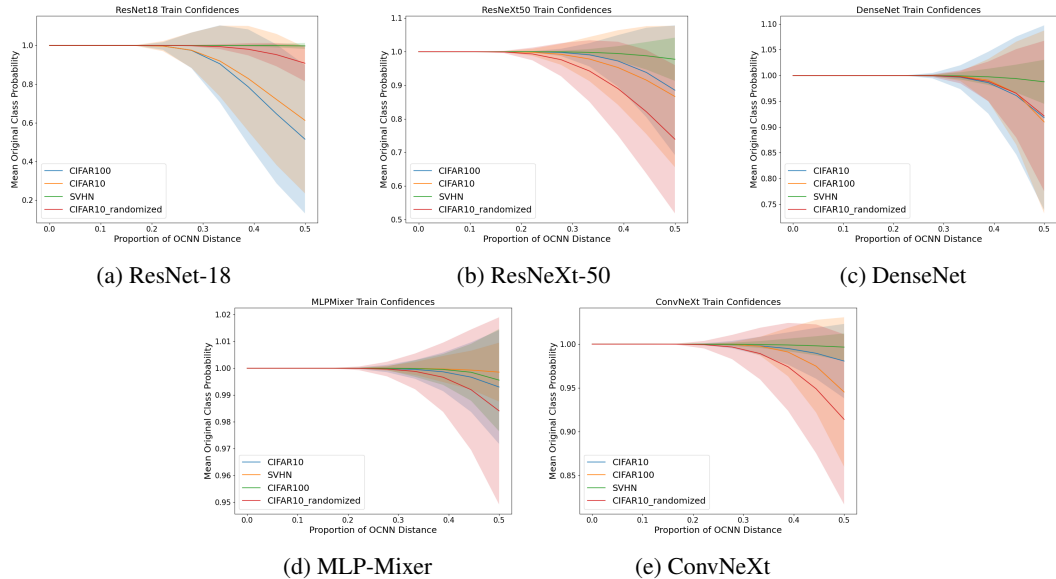


Figure 2: Mean original class softmax outputs across various neighborhood sizes for different models trained with *empirical risk minimization*, as described in our experimental setup. The shaded regions around each curve represent one standard deviation.

As discussed in Section 1, this kind of model behavior can have significant consequences for critical use cases, so it is desirable to have a means of mitigating it. We will show in Section 4, however, that uniform confidence cannot be handled in certain cases by post-training calibration methods.

Instead, we need to rely on preventing uniform confidence entirely by modifying the training process of the model. We focus on one particular training modification - Mixup data-augmentation (Zhang et al., 2017b) - which simply requires training models on random convex combinations of the original data points and their labels (see Section 3.3 for precise details). Mixup has been shown to appropriately decrease model confidence (Thulasidasan et al., 2019), and we confirm these findings in our setting by repeating our experiments but training using Mixup with a uniform mixing distribution, with corresponding results shown in Figure 3.

As can be seen from comparing Figures 2 and 3, training with Mixup clearly avoids the uniform confidence phenomenon. In the rest of this work, we focus on developing theory to explain why this happens and when the regularization introduced by Mixup is useful with respect to calibration. The key idea is that Mixup *constrains model behavior away from the training data*.

Further Experiments. In addition to the experiments in this section, we also: explore how the logits of all of the models considered in Figures 2 and 3 behave (Appendix B.1), analyze the impact of training horizon on uniform confidence (Appendix B.2), evaluate confidence on test data (Appendix B.3), and verify consistency of our findings for larger datasets (Appendix B.4).

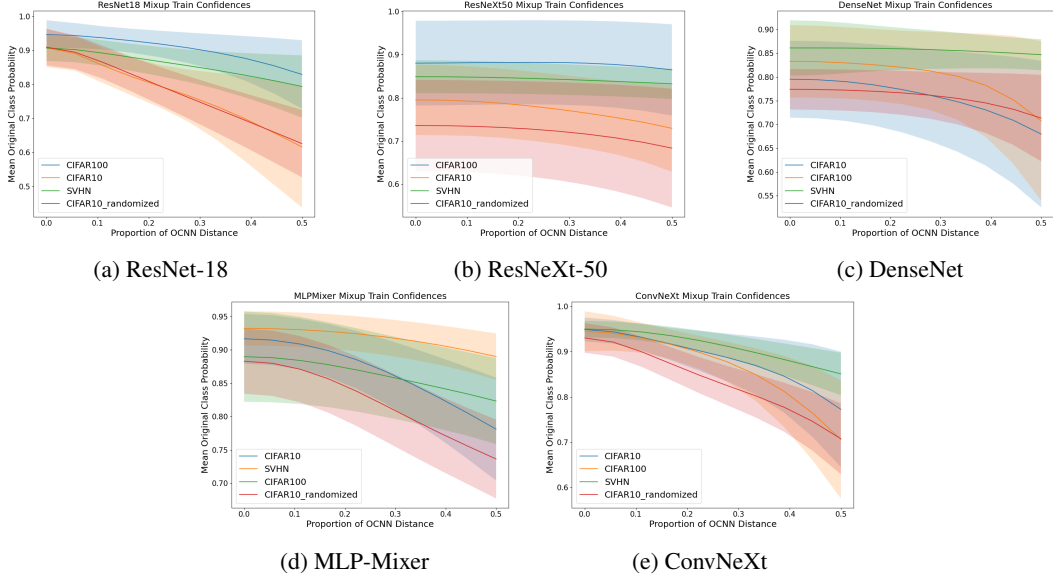


Figure 3: A replication of the experiments from Figure 2, but training using *Mixup* (uniform mixing distribution) instead of empirical risk minimization.

2.1 Dataset and Model Details

Datasets. We consider the standard image classification benchmarks of CIFAR-10, CIFAR-100, and SVHN downsampled (uniformly at random) to consist of 5000 training data points. Additionally, we also consider a version of CIFAR-10 with entirely randomized labels (“CIFAR10_randomized” in Figures 2 and 3), as was done by Zhang et al. (2017a), in order to examine whether data/label relationships have any influence on our results. We preprocess all datasets to have zero mean and unit variance, and maintain the original input resolution ($3 \times 32 \times 32$ size images). This ensures that 5000 data points are enough to avoid trivial linear separability of each dataset.

Models. We train ResNet-18 (He et al., 2015), ResNeXt-50 (Xie et al., 2016), DenseNet (Huang et al., 2016), MLP-Mixer (Tolstikhin et al., 2021), and ConvNeXt (Liu et al., 2022) architectures on all of the aforementioned datasets. We use the popular PyTorch (Paszke et al., 2019) open source implementations (MIT license) of Kuang Liu and Phil Wang for ResNet-18 and MLP-Mixer respectively, and for MLP-Mixer we use a patch size of 8×8 , a depth of 8, and a hidden layer dimension of 1024 (this is smaller than any model considered in the original paper). We use ResNeXt 32×4 , DenseNet-121, and ConvNeXt-Tiny (with untrained weights) as provided in PyTorch.

Training Details. All models were trained for 500 epochs using Adam (Kingma & Ba, 2015) with the standard hyperparameters of $\beta_1 = 0.9$, $\beta_2 = 0.999$, a learning rate of 0.001, and a batch size of 500 on a single A5000 GPU. We did not use any additional training heuristics such as Dropout (Srivastava et al., 2014). In preliminary experiments, we found that changes to optimizer/learning rate did not influence our results so long as the training horizon was sufficiently large for achieving interpolation (zero training error) on the training data.

3 Theoretical Preliminaries

Notation. We use $[k]$ to denote $\{1, 2, \dots, k\}$ for a positive integer k . We consider k -class classification and use \mathcal{X} to denote a dataset of N points (x_i, y_i) sampled from a distribution $\pi(X, Y)$ whose support $\text{supp}(\pi)$ is contained in $\mathbb{R}^d \times [k]$. We use π_X and π_Y to denote the respective marginal distributions of π , and use π_y to denote the conditional distribution $\pi(X \mid Y = y)$. We use $d(A, B)$ to denote the Euclidean distance between two sets $A, B \subset \mathbb{R}^d$, $d_{\text{KL}}(\pi_1, \pi_2)$ to denote the KL divergence between two distributions π_1 and π_2 , and μ_d for the Lebesgue measure on \mathbb{R}^d . For a function $g : \mathbb{R}^d \rightarrow \mathbb{R}^k$, we use g^i to denote the i^{th} coordinate function of g . Lastly, we use $\phi(\cdot)$ to denote the softmax function,

i.e. $\phi^i(g(x)) = \exp(g^i(x)) / \sum_{j \in [k]} \exp(g^j(x))$. In everything that follows, we assume both N and k are sufficiently large, and that $N = \Omega(\text{poly}(k))$ for some large degree polynomial $\text{poly}(k)$.

3.1 Calibration

In training a model g on a dataset \mathcal{X} , the goal is for $\phi^Y(g(X))$ to recover the ground truth conditional distribution $\pi(Y | X)$. However, this is usually unattainable when training on finite datasets. We may thus hope instead to satisfy the weaker property that the trained model g is *calibrated*, which can be formulated as the following regular conditional probability condition:

$$\mathbb{P}(Y = y | \phi^y(g(X)) = p_y) = p_y \quad (3.1)$$

Equation (3.1) captures the earlier mentioned intuition that, when our model predicts probability p_y for a class y , the true probability for the class y (for those predicted instances) is also p_y . It is straightforward to translate Equation (3.1) into a notion of miscalibration by considering the expectation of the absolute difference between the left and right-hand sides; this is the expected calibration error (ECE). Although natural, ECE suffers from several theoretical and empirical drawbacks (Błasior et al., 2023), and we opt to instead work with the expected KL divergence $\mathbb{E}_{X \sim \pi_X} [d_{\text{KL}}(\pi(Y | X), \cdot)]$, as minimizing this implies that Equation (3.1) is satisfied (and importantly, we will consider theoretical settings in which we allow post-training calibration methods access to π).

With a notion of miscalibration in hand, we consider methods to improve the calibration of a trained model g . One of the most popular (and simplest) approaches is temperature scaling (Guo et al., 2017), which consists of introducing a single parameter T that is used to scale the outputs of g . The value of T is obtained by optimizing the negative log-likelihood on a calibration dataset \mathcal{X}_{cal} :

$$T = \underset{\hat{T} \in (0, \infty)}{\operatorname{argmin}} - \frac{1}{|\mathcal{X}_{\text{cal}}|} \sum_{(x_i, y_i) \in \mathcal{X}_{\text{cal}}} \log \phi^{y_i}(g(x_i) / \hat{T}) \quad (3.2)$$

For our results, we will in fact consider an even more powerful (and impractical) form of temperature scaling in which we allow access to the ground-truth distribution π :

$$T = \underset{\hat{T} \in (0, \infty)}{\operatorname{argmin}} \mathbb{E}_{X \sim \pi_X} \left[d_{\text{KL}}(\pi(Y | X), \phi^Y(g(X) / \hat{T})) \right] \quad (3.3)$$

We will henceforth refer to an optimally temperature-scaled model with respect to Equation (3.3) as g_T . We will show in Section 4 that even when we allow this “oracle” temperature scaling, we cannot hope to calibrate models g that exhibit the uniform confidence behavior discussed in Section 2.

3.2 Empirical Risk Minimization

In practice, models are often trained via empirical risk minimization (ERM). Due to the large number of parameters in modern models, training often leads to an *interpolator* that is very confident on every training data point $(x_i, y_i) \in \mathcal{X}$, as we formalize below:

Definition 3.1. [ERM Interpolator] For a dataset \mathcal{X} , we say that a model g is an ERM interpolator if for every $(x_i, y_i) \in \mathcal{X}$ there exists a universal constant C_i such that:

$$\min_{s \neq y_i} g^{y_i}(x_i) - g^s(x_i) > \log k \quad \text{and} \quad \max_{r, s \neq y_i} g^s(x_i) - g^r(x_i) < C_i \quad (3.4)$$

Equation (3.4) is slightly stronger than directly assuming $\phi^{y_i}(g(x_i)) \approx 1$; it is motivated by further empirical analysis in Appendix B.1, in which we show that the logits associated with incorrect classes on the training data for the models in Section 2 are near zero. We now also introduce a direct theoretical analogue to the uniform confidence behavior in Section 2.

Definition 3.2. [Uniform γ -Confidence] For a point $(x_i, y_i) \in \mathcal{X}$, letting L be a universal constant, we define:

$$\mathcal{B}_\gamma(x_i) = \{x \in \mathbb{R}^d : \|x_i - x\| \leq \gamma\} \quad (3.5)$$

$$\mathcal{G}_\gamma(x_i) = \{x \in \mathbb{R}^d : |g^{y_i}(x_i) - g^{y_i}(x)| \leq L\gamma\} \quad (3.6)$$

We say that a model g is uniformly γ -confident over a set U if there exists a class $y \in [k]$ and $\Theta(N/k)$ points $(x_i, y) \in \mathcal{X}$ with $x_i \in U$ such that $\pi_y(X \in \mathcal{G}_\gamma(x_i) | X \in \mathcal{B}_\gamma(x_i)) \geq 1 - O(1/k)$.

Basically, Definition 3.2 codifies the idea that the model logit g^{y_i} does not change much in a small enough neighborhood of each x_i in a set U , with high probability. We will show in Theorem 4.5 that satisfying Definitions 3.1 and 3.2 is sufficient for poor calibration for a wide class of data distributions, even when using temperature scaling with access to the ground truth distribution oracle.

3.3 Mixup

In contrast, we can show that if we consider models minimizing a Mixup-like training objective instead of the usual negative log-likelihood in Equation (3.2), we can avoid uniform confidence.

Let \mathcal{D}_λ denote a continuous distribution supported on $[0, 1]$ and let $z_{i,j}(\lambda) = \lambda x_i + (1 - \lambda)x_j$ (using $z_{i,j}$ when λ is clear from context) where $(x_i, y_i), (x_j, y_j) \in \mathcal{X}$. Then we may define the empirical Mixup cross-entropy $J_{\text{mix}}(g, \mathcal{X}, \mathcal{D}_\lambda)$ as:

$$J_{\text{mix}}(g, \mathcal{X}, \mathcal{D}_\lambda) = -\frac{1}{N^2} \sum_{i \in [N]} \sum_{j \in [N]} \mathbb{E}_{\lambda \sim \mathcal{D}_\lambda} [\lambda \log \phi^{y_i}(g(z_{i,j})) + (1 - \lambda) \log \phi^{y_j}(g(z_{i,j}))] \quad (3.7)$$

Essentially, minimizing Equation (3.7) forces a model to linearly interpolate between its predictions $\phi^{y_i}(g(x_i))$ and $\phi^{y_j}(g(x_j))$ over the line segment connecting the points x_i and x_j . This already provides some intuition for why Mixup-optimal models will fail to satisfy a property like uniform γ -confidence from Definition 3.2: *their behavior is constrained away from the training data*.

However, the line segment constraints of $J_{\text{mix}}(g, \mathcal{X}, \mathcal{D}_\lambda)$ will not be enough to make this intuition rigorous when the data is in \mathbb{R}^d with $d > 1$, since in this case line segments are measure zero sets with respect to μ_d . We will thus augment Mixup to work with convex combinations of $d + 1$ points as opposed to two, and refer to this new objective as **d -Mixup**.

In generalizing from Mixup to d -Mixup, it is helpful from a theoretical standpoint to constrain the set of allowed mixings $\mathcal{M}_d(\mathcal{X}) \subset [N]^{d+1}$. We will consider only mixing points at most some constant distance away from one another, and we will also preclude mixing points that are too highly correlated.¹ The precise definition of $\mathcal{M}_d(\mathcal{X})$ can be found in Definition A.1 of Appendix A.2; we omit it here due to its technical nature.

Now let $\mathcal{D}_{\lambda,d}$ denote a continuous distribution supported on the d -dimensional probability simplex $\Delta^d \subset \mathbb{R}^{d+1}$. Defining $z_\sigma(\lambda) = \sum_{j \in [d+1]} \lambda_j x_{\sigma_j}$ for $\lambda \in \text{supp}(\mathcal{D}_{\lambda,d})$ and $\sigma \in \mathcal{M}_d(\mathcal{X})$, we can define the empirical d -Mixup cross-entropy $J_{\text{mix},d}(g, \mathcal{X}, \mathcal{D}_{\lambda,d})$:

$$J_{\text{mix},d}(g, \mathcal{X}, \mathcal{D}_{\lambda,d}) = -\frac{1}{|\mathcal{M}_d(\mathcal{X})|} \sum_{\sigma \in \mathcal{M}_d(\mathcal{X})} \mathbb{E}_{\lambda \sim \mathcal{D}_{\lambda,d}} \left[\sum_{j \in [d+1]} \lambda_j \log \phi^{y_{\sigma_j}}(g(z_\sigma(\lambda))) \right] \quad (3.8)$$

We will henceforth use $\mathcal{X}_{\text{mix},d}$ to denote the set of all z_σ . The main benefit of introducing the set $\mathcal{M}_d(\mathcal{X})$ instead of just generalizing Equation (3.7) to mixing over $[N]^{d+1}$ is that it allows us to use a reparameterization trick with which we can characterize the d -Mixup optimal prediction at every mixed point z_σ . We state only an informal version of this result below and defer a formal statement and proof to Appendix A.2.

Lemma 3.3. [Informal Optimality Lemma] Every $g^* \in \text{arginf}_g J_{\text{mix},d}(g, \mathcal{X}, \mathcal{D}_{\lambda,d})$ (where the arginf is over all extended \mathbb{R}^d -valued functions) satisfies $\phi^y(g^*(z)) = \alpha_y(z) / \sum_{s \in [k]} \alpha_s(z)$ for almost every $z_\sigma \in \mathcal{X}_{\text{mix},d}$, where $\alpha_y(z)$ corresponds to the expected weight of class y points over all mixing sets $\sigma \in \mathcal{M}_d(\mathcal{X})$ from which we can obtain z .

We note that this lemma is analogous to Lemma 2.3 in the work of Chidambaram et al. (2021), but avoids restrictions on the function class being considered and is non-asymptotic. Since we can characterize optimal predictions over $\mathcal{X}_{\text{mix},d}$, we can define d -Mixup interpolators as follows.

Definition 3.4. [d -Mixup Interpolator] For a dataset \mathcal{X} , we say that g is a d -Mixup interpolator if $\phi^y(g(z)) = \phi^y(g^*(z)) \pm O(1/k)$ for almost every $z \in \mathcal{X}_{\text{mix},d}$ and $y \in [k]$, with $g^* \in \text{arginf}_g J_{\text{mix},d}(g, \mathcal{X}, \mathcal{D}_{\lambda,d})$.

¹This means we do not mix points with themselves in d -Mixup; however, when π_X has a density, this makes little difference since we can mix in a neighborhood of any point.

In Theorem 4.6, we will show that d -Mixup interpolators can achieve good calibration on a subclass of distributions for which ERM interpolators perform poorly.

Remark 3.5. In practice it is unreasonable to mix $d + 1$ points when d is large. However, we conjecture that due to the regularity of practical models (i.e. neural networks), even mixing two points as in traditional Mixup is sufficient for achieving neighborhood constraints like those induced by d -Mixup, hence the results of Figure 3. We introduce d -Mixup because we make no such regularity assumptions on the models in our theory.

4 Theoretical Implications of the Uniform Confidence Phenomenon

In this section, we show that even for simple data distributions, uniform confidence can prevent post-training calibration methods (temperature scaling) from producing well-calibrated models, while modifications in the training process (Mixup) can potentially address this issue. Prior to proving our main results, we begin first with a 1-dimensional example that contains the key ideas of our analysis. The full proofs of all results in this section can be found in Appendix A.

4.1 Warm-Up: A Simple 1-D Example

Definition 4.1. [Overlapping Intervals] Let $\tau(y)$ denote the parity of a nonnegative integer y and let $\beta_y = \lfloor (y-1)/2 \rfloor k + \tau(y-1)$ for $y \in [k]$. Then we define $\pi(X, Y)$ to be the distribution on $\mathbb{R} \times [k]$ such that π_Y is uniform over $[k]$ and $\pi(X | Y = y)$ is uniform over $[\beta_y, \beta_y + 2]$.

Definition 4.1 corresponds to a distribution in which consecutive class-conditional densities are supported on overlapping intervals of length 2 (starting from 0) with a spacing of k between each pair of classes (see Figure 4).

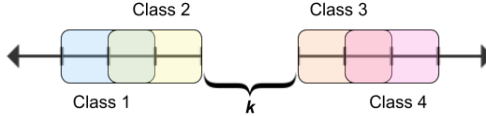


Figure 4: Visualization of Definition 4.1 for the case $k = 4$.

The idea is that ERM interpolators for \mathcal{X} that are uniformly confident will be poorly calibrated in each overlapping region in the support of π_X . This is made precise in the following proposition.

Proposition 4.2. Let \mathcal{X} consist of N i.i.d. draws from the distribution π specified in Definition 4.1. Then with probability at least $1 - k \exp(-\Omega(N/k))$ over the randomness of \mathcal{X} , the set \mathcal{S} of all models g that are ERM interpolators for \mathcal{X} and uniformly $k/(2N)$ -confident over each overlapping region in $\text{supp}(\pi_X)$ is non-empty (in fact, uncountable). Furthermore, the predictive distribution $\hat{\pi}_T(Y | X) = \phi^Y(g_T(X))$ of the optimally temperature-scaled model g_T for any $g \in \mathcal{S}$ satisfies:

$$\mathbb{E}_{X \sim \pi_X} [d_{\text{KL}}(\pi(Y | X), \hat{\pi}_T(Y | X))] \geq \Theta(\log k) \quad (4.1)$$

In other words, even with temperature scaling every $g \in \mathcal{S}$ is asymptotically no better than random.

Proof Sketch. We can show that \mathcal{S} is non-trivial using Chernoff bound arguments, and then use uniform confidence to show that there is a significant fraction of $\text{supp}(\pi_X)$ on which every $g \in \mathcal{S}$ predicts incorrect probabilities. The key idea is then that temperature scaling will only improve incorrect predictions for ERM interpolators to uniformly random (i.e. $1/k$), whereas the correct prediction in an overlapping region is $1/2$ for each of the overlapping classes.

On the other hand, for d -Mixup, each point in the overlapping regions can be obtained as a mixture of points from the overlapping classes, so we will have non-trivial probabilities for both classes.

Proposition 4.3. Let \mathcal{X} be as in Proposition 4.2 and $p(k)$ denote a polynomial in k of degree at least one. Then taking $\mathcal{D}_{\lambda,1}$ to be uniform, every 1-Mixup interpolator g for \mathcal{X} with the property that $\phi^y(g(x)) \leq 1 - \Omega(1/p(k))$ for every $x \in \text{supp}(\pi_X) \setminus \mathcal{X}_{\text{mix},1}$ and $y \in [k]$ satisfies with probability at least $1 - k^2 \exp(-\Omega(N/k^2))$:

$$\mathbb{E}_{X \sim \pi_X} [d_{\text{KL}}(\pi(Y | X), \hat{\pi}(Y | X))] \leq \Theta(1) \quad (4.2)$$

Proof Sketch. We can show with high probability that $\mathcal{X}_{\text{mix},1}$ covers most of $\text{supp}(\pi_X)$ uniformly, and then we can use Lemma 3.3 to precisely characterize the 1-Mixup predictions over $\mathcal{X}_{\text{mix},1}$.

We needed to add the (relatively weak) stipulation that $\phi^y(g(x)) \leq 1 - \Omega(1/\text{poly}(k))$ in the statement above, since we cannot hope to prove an upper bound if g is allowed to behave arbitrarily on $\text{supp}(\pi_X) \setminus \mathcal{X}_{\text{mix},1}$.

4.2 Generalizing to Higher Dimensions

By extending the idea of overlapping regions in $\text{supp}(\pi_X)$ from our 1-D example, we can generalize the failure of ERM interpolators to higher-dimensional distributions.

Definition 4.4. [General Data Distribution] We define π to be any distribution whose support is contained in $\mathbb{R}^d \times [k]$ satisfying the following constraints:

1. (Classes are roughly balanced) $\pi_Y(Y = y) = \Theta(1/k)$.
2. (Constant class overlaps) Letting M denote a nonnegative integer constant, there exist $\Theta(k)$ classes y for which there are classes $s_1(y), s_2(y), \dots, s_m(y)$ for some $1 \leq m < M$ with $\pi_X(\text{supp}(\pi_y) \cap \text{supp}(\pi_{s_i(y)})) \geq C$ for a universal constant $C > 0$, and all other $s' \in [k]$ satisfy $\pi_X(\text{supp}(\pi_y) \cap \text{supp}(\pi_{s'})) = 0$.
3. (Overlap density is proportional to measure) $\pi_y(X \in A) = \Theta(\mu_d(A))$ and $\pi_{s_i(y)}(X \in A) = \Theta(\mu_d(A))$ for every $A \subseteq \text{supp}(\pi_y) \cap \text{supp}(\pi_{s_i(y)})$.

Definition 4.4 is quite broad in that we make no assumptions on the behavior of the class-conditional densities outside of the overlapping regions. We now generalize Proposition 4.2.

Theorem 4.5. Let \mathcal{X} consist of N i.i.d. draws from any distribution π satisfying Definition 4.4, and let $r \in \mathbb{R}$ be such that the sphere with radius r in \mathbb{R}^d has volume $k/(MN)$. Then the result of Proposition 4.2 still holds for the set \mathcal{S}_d of ERM interpolators for \mathcal{X} which are uniformly r -confident over each overlapping region in $\text{supp}(\pi_X)$.

To generalize Proposition 4.3, however, we need further restrictions on π . Mainly, we need to have significant spacing between non-overlapping classes (as in Definition 4.1), and we need to restrict the class-conditional densities such that mixings in $\mathcal{X}_{\text{mix},d}$ are not too skewed towards a small subset of classes. The precise formulation of this assumption can be found in Appendix A.2.

Theorem 4.6. Let \mathcal{X} consist of N i.i.d. draws from any distribution π satisfying Definition 4.4 and Assumption A.3, and let $p(k)$ be as in Proposition 4.3. Then the result of Proposition 4.3 still holds when considering d -Mixup interpolators g for \mathcal{X} where the mixing distribution $\mathcal{D}_{\lambda,d}$ is uniform over the d -dimensional probability simplex.

5 Limitations and Discussion

Limitations. Perhaps the main empirical limitation of our work is the reliance on subsampling due to computational constraints in the experiments of Section 2, and it may be interesting in future work to explore properties of the OCNN distance for larger-scale datasets. However, as mentioned in Section 2, our further experiments in Appendix B suggest that our findings should generalize.

On the theoretical side, the main limitation is technicalities introduced due to d -Mixup. Namely, it becomes very difficult to reason about what the set of d -Mixup points $\mathcal{X}_{\text{mix},d}$ looks like in high dimensions, thereby forcing parts of our theory to directly assume some high probability behavior of $\mathcal{X}_{\text{mix},d}$ (justified by the simple example in Definition 4.1).

Discussion. The key findings of our work are that trained neural networks can exhibit large regions of near-certain confidence around their training points, and that when this behavior occurs we cannot hope to fix calibration for data distributions with class overlaps using temperature-scaling-type methods. One clear direction suggested by our work is the idea of developing better *neighborhood constraints* around training points; we study the constraints introduced by Mixup, but we anticipate there are likely better alternatives for improving calibration. For broader impacts, the main concern introduced by our work is that critical use cases (i.e. medical applications) may be significantly impacted by the uniform confidence phenomenon of Section 2 - we hope that this initial work instigates further studies into how models can be improved for such use cases.

Acknowledgements

Rong Ge and Muthu Chidambaram are supported by NSF Award DMS-2031849, CCF-1845171 (CAREER), CCF-1934964 (Tripods), and a Sloan Research Fellowship. Muthu would like to thank Kai Xu for helpful discussions during the early stages of this project.

References

- Bojarski, M., Testa, D. D., Dworakowski, D., Firner, B., Flepp, B., Goyal, P., Jackel, L. D., Monfort, M., Muller, U., Zhang, J., Zhang, X., Zhao, J., and Zieba, K. End to end learning for self-driving cars, 2016.
- Błasior, J., Gopalan, P., Hu, L., and Nakkiran, P. A unifying theory of distance from calibration, 2023.
- Carlini, N. and Wagner, D. Towards evaluating the robustness of neural networks, 2017.
- Chidambaram, M., Wang, X., Hu, Y., Wu, C., and Ge, R. Towards understanding the data dependency of mixup-style training. *CoRR*, abs/2110.07647, 2021. URL <https://arxiv.org/abs/2110.07647>.
- Clements, J. M., Xu, D., Yousefi, N., and Efimov, D. Sequential deep learning for credit risk monitoring with tabular financial data, 2020.
- Ding, Z., Han, X., Liu, P., and Niethammer, M. Local temperature scaling for probability calibration. *CoRR*, abs/2008.05105, 2020. URL <https://arxiv.org/abs/2008.05105>.
- Elmarakeby, H. A., Hwang, J., Arafeh, R., Crowdus, J., Gang, S., Liu, D., AlDubayan, S. H., Salari, K., Kregel, S., Richter, C., et al. Biologically informed deep neural network for prostate cancer discovery. *Nature*, 598(7880):348–352, 2021.
- Esteva, A., Kuprel, B., Novoa, R. A., Ko, J., Swetter, S. M., Blau, H. M., and Thrun, S. Dermatologist-level classification of skin cancer with deep neural networks. *nature*, 542(7639):115–118, 2017.
- Esteva, A., Chou, K., Yeung, S., Naik, N., Madani, A., Mottaghi, A., Liu, Y., Topol, E., Dean, J., and Socher, R. Deep learning-enabled medical computer vision. *NPJ digital medicine*, 4(1):5, 2021.
- Grigorescu, S., Trasnea, B., Cocias, T., and Macesanu, G. A survey of deep learning techniques for autonomous driving. *Journal of Field Robotics*, 37(3):362–386, 2020.
- Guo, C., Pleiss, G., Sun, Y., and Weinberger, K. Q. On calibration of modern neural networks. In *Proceedings of the 34th International Conference on Machine Learning - Volume 70*, ICML’17, pp. 1321–1330. JMLR.org, 2017.
- He, K., Zhang, X., Ren, S., and Sun, J. Deep residual learning for image recognition. *CoRR*, abs/1512.03385, 2015. URL <http://arxiv.org/abs/1512.03385>.
- Hein, M., Andriushchenko, M., and Bitterwolf, J. Why relu networks yield high-confidence predictions far away from the training data and how to mitigate the problem. In *IEEE Conference on Computer Vision and Pattern Recognition, CVPR 2019, Long Beach, CA, USA, June 16-20, 2019*, pp. 41–50. Computer Vision Foundation / IEEE, 2019. doi: 10.1109/CVPR.2019.00013. URL http://openaccess.thecvf.com/content_CVPR_2019/html/Hein_Why_ReLU_Networks_Yield_High-Confidence_Predictions_Far_Away_From_the_CVPR_2019_paper.html.
- Huang, G., Liu, Z., and Weinberger, K. Q. Densely connected convolutional networks. *CoRR*, abs/1608.06993, 2016. URL <http://arxiv.org/abs/1608.06993>.
- Jiang, X., Osl, M., Kim, J., and Ohno-Machado, L. Calibrating predictive model estimates to support personalized medicine. *Journal of the American Medical Informatics Association*, 19(2):263–274, 2012.

- Kingma, D. P. and Ba, J. Adam: A method for stochastic optimization. In Bengio, Y. and LeCun, Y. (eds.), *3rd International Conference on Learning Representations, ICLR 2015, San Diego, CA, USA, May 7-9, 2015, Conference Track Proceedings*, 2015. URL <http://arxiv.org/abs/1412.6980>.
- Kristiadi, A., Hein, M., and Hennig, P. Being bayesian, even just a bit, fixes overconfidence in relu networks, 2020.
- Kull, M., Perelló-Nieto, M., Kängsepp, M., de Menezes e Silva Filho, T., Song, H., and Flach, P. A. Beyond temperature scaling: Obtaining well-calibrated multiclass probabilities with dirichlet calibration. *CoRR*, abs/1910.12656, 2019. URL <http://arxiv.org/abs/1910.12656>.
- Kumar, A., Sarawagi, S., and Jain, U. Trainable calibration measures for neural networks from kernel mean embeddings. In Dy, J. and Krause, A. (eds.), *Proceedings of the 35th International Conference on Machine Learning*, volume 80 of *Proceedings of Machine Learning Research*, pp. 2805–2814. PMLR, 10–15 Jul 2018. URL <https://proceedings.mlr.press/v80/kumar18a.html>.
- Lakshminarayanan, B., Pritzel, A., and Blundell, C. Simple and scalable predictive uncertainty estimation using deep ensembles, 2017.
- Liu, Z., Mao, H., Wu, C., Feichtenhofer, C., Darrell, T., and Xie, S. A convnet for the 2020s. *CoRR*, abs/2201.03545, 2022. URL <https://arxiv.org/abs/2201.03545>.
- Meinke, A. and Hein, M. Towards neural networks that provably know when they don't know. In *8th International Conference on Learning Representations, ICLR 2020, Addis Ababa, Ethiopia, April 26-30, 2020*. OpenReview.net, 2020. URL <https://openreview.net/forum?id=ByxGkySKwH>.
- Minderer, M., Djolonga, J., Romijnders, R., Hubis, F., Zhai, X., Houlsby, N., Tran, D., and Lucic, M. Revisiting the calibration of modern neural networks. In Ranzato, M., Beygelzimer, A., Dauphin, Y., Liang, P., and Vaughan, J. W. (eds.), *Advances in Neural Information Processing Systems*, volume 34, pp. 15682–15694. Curran Associates, Inc., 2021. URL https://proceedings.neurips.cc/paper_files/paper/2021/file/8420d359404024567b5aefda1231af24-Paper.pdf.
- Müller, R., Kornblith, S., and Hinton, G. When does label smoothing help?, 2020.
- Ovadia, Y., Fertig, E., Ren, J., Nado, Z., Sculley, D., Nowozin, S., Dillon, J., Lakshminarayanan, B., and Snoek, J. Can you trust your model's uncertainty? evaluating predictive uncertainty under dataset shift. In Wallach, H., Larochelle, H., Beygelzimer, A., d'Alché-Buc, F., Fox, E., and Garnett, R. (eds.), *Advances in Neural Information Processing Systems*, volume 32. Curran Associates, Inc., 2019. URL https://proceedings.neurips.cc/paper_files/paper/2019/file/8558cb408c1d76621371888657d2eb1d-Paper.pdf.
- Paszke, A., Gross, S., Massa, F., Lerer, A., Bradbury, J., Chanan, G., Killeen, T., Lin, Z., Gimelshein, N., Antiga, L., Desmaison, A., Köpf, A., Yang, E. Z., DeVito, Z., Raison, M., Tejani, A., Chilamkurthy, S., Steiner, B., Fang, L., Bai, J., and Chintala, S. Pytorch: An imperative style, high-performance deep learning library. *CoRR*, abs/1912.01703, 2019. URL <http://arxiv.org/abs/1912.01703>.
- Srivastava, N., Hinton, G., Krizhevsky, A., Sutskever, I., and Salakhutdinov, R. Dropout: A simple way to prevent neural networks from overfitting. *Journal of Machine Learning Research*, 15(56):1929–1958, 2014. URL <http://jmlr.org/papers/v15/srivastava14a.html>.
- Thulasidasan, S., Chennupati, G., Bilmes, J. A., Bhattacharya, T., and Michalak, S. On mixup training: Improved calibration and predictive uncertainty for deep neural networks. *Advances in Neural Information Processing Systems*, 32:13888–13899, 2019.
- Tolstikhin, I. O., Houlsby, N., Kolesnikov, A., Beyer, L., Zhai, X., Unterthiner, T., Yung, J., Steiner, A., Keysers, D., Uszkoreit, J., Lucic, M., and Dosovitskiy, A. Mlp-mixer: An all-mlp architecture for vision. *CoRR*, abs/2105.01601, 2021. URL <https://arxiv.org/abs/2105.01601>.

- Wang, D.-B., Feng, L., and Zhang, M.-L. Rethinking calibration of deep neural networks: Do not be afraid of overconfidence. In Ranzato, M., Beygelzimer, A., Dauphin, Y., Liang, P., and Vaughan, J. W. (eds.), *Advances in Neural Information Processing Systems*, volume 34, pp. 11809–11820. Curran Associates, Inc., 2021. URL https://proceedings.neurips.cc/paper_files/paper/2021/file/61f3a6dbc9120ea78ef75544826c814e-Paper.pdf.
- Wen, Y., Tran, D., and Ba, J. Batchensemble: An alternative approach to efficient ensemble and lifelong learning, 2020.
- Wen, Y., Jerfel, G., Muller, R., Dusenberry, M. W., Snoek, J., Lakshminarayanan, B., and Tran, D. Combining ensembles and data augmentation can harm your calibration, 2021.
- Xie, S., Girshick, R. B., Dollár, P., Tu, Z., and He, K. Aggregated residual transformations for deep neural networks. *CoRR*, abs/1611.05431, 2016. URL <http://arxiv.org/abs/1611.05431>.
- Zhang, C., Bengio, S., Hardt, M., Recht, B., and Vinyals, O. Understanding deep learning requires rethinking generalization, 2017a.
- Zhang, H., Cissé, M., Dauphin, Y. N., and Lopez-Paz, D. mixup: Beyond empirical risk minimization. *CoRR*, abs/1710.09412, 2017b. URL <http://arxiv.org/abs/1710.09412>.
- Zhang, L., Deng, Z., Kawaguchi, K., and Zou, J. When and how mixup improves calibration. *CoRR*, abs/2102.06289, 2021. URL <https://arxiv.org/abs/2102.06289>.

A Full Proofs

Here we provide full proofs of all results in Section 4. For convenience, we first recall all of the relevant definitions and assumptions from Sections 3 and 4.

Definition 3.1. [ERM Interpolator] For a dataset \mathcal{X} , we say that a model g is an ERM interpolator if for every $(x_i, y_i) \in \mathcal{X}$ there exists a universal constant C_i such that:

$$\min_{s \neq y_i} g^{y_i}(x_i) - g^s(x_i) > \log k \quad \text{and} \quad \max_{r, s \neq y_i} g^s(x_i) - g^r(x_i) < C_i \quad (3.4)$$

Definition 3.2. [Uniform γ -Confidence] For a point $(x_i, y_i) \in \mathcal{X}$, letting L be a universal constant, we define:

$$\mathcal{B}_\gamma(x_i) = \{x \in \mathbb{R}^d : \|x_i - x\| \leq \gamma\} \quad (3.5)$$

$$\mathcal{G}_\gamma(x_i) = \{x \in \mathbb{R}^d : |g^{y_i}(x_i) - g^{y_i}(x)| \leq L\gamma\} \quad (3.6)$$

We say that a model g is uniformly γ -confident over a set U if there exists a class $y \in [k]$ and $\Theta(N/k)$ points $(x_i, y) \in \mathcal{X}$ with $x_i \in U$ such that $\pi_y(X \in \mathcal{G}_\gamma(x_i) \mid X \in \mathcal{B}_\gamma(x_i)) \geq 1 - O(1/k)$.

Definition 3.4. [d -Mixup Interpolator] For a dataset \mathcal{X} , we say that g is a d -Mixup interpolator if $\phi^y(g(z)) = \phi^y(g^*(z)) \pm O(1/k)$ for almost every $z \in \mathcal{X}_{\text{mix},d}$ and $y \in [k]$, with $g^* \in \arg\inf_g J_{\text{mix},d}(g, \mathcal{X}, \mathcal{D}_{\lambda,d})$.

Definition 4.1. [Overlapping Intervals] Let $\tau(y)$ denote the parity of a nonnegative integer y and let $\beta_y = \lfloor (y-1)/2 \rfloor k + \tau(y-1)$ for $y \in [k]$. Then we define $\pi(X, Y)$ to be the distribution on $\mathbb{R} \times [k]$ such that π_Y is uniform over $[k]$ and $\pi(X \mid Y = y)$ is uniform over $[\beta_y, \beta_y + 2]$.

Definition 4.4. [General Data Distribution] We define π to be any distribution whose support is contained in $\mathbb{R}^d \times [k]$ satisfying the following constraints:

1. (Classes are roughly balanced) $\pi_Y(Y = y) = \Theta(1/k)$.
2. (Constant class overlaps) Letting M denote a nonnegative integer constant, there exist $\Theta(k)$ classes y for which there are classes $s_1(y), s_2(y), \dots, s_m(y)$ for some $1 \leq m < M$ with $\pi_X(\text{supp}(\pi_y) \cap \text{supp}(\pi_{s_i(y)})) \geq C$ for a universal constant $C > 0$, and all other $s' \in [k]$ satisfy $\pi_X(\text{supp}(\pi_y) \cap \text{supp}(\pi_{s'})) = 0$.
3. (Overlap density is proportional to measure) $\pi_y(X \in A) = \Theta(\mu_d(A))$ and $\pi_{s_i(y)}(X \in A) = \Theta(\mu_d(A))$ for every $A \subseteq \text{supp}(\pi_y) \cap \text{supp}(\pi_{s_i(y)})$.

A.1 Proofs of Proposition 4.2 and Theorem 4.5

Proposition 4.2. Let \mathcal{X} consist of N i.i.d. draws from the distribution π specified in Definition 4.1. Then with probability at least $1 - k \exp(-\Omega(N/k))$ over the randomness of \mathcal{X} , the set \mathcal{S} of all models g that are ERM interpolators for \mathcal{X} and uniformly $k/(2N)$ -confident over each overlapping region in $\text{supp}(\pi_X)$ is non-empty (in fact, uncountable). Furthermore, the predictive distribution $\hat{\pi}_T(Y \mid X) = \phi^Y(g_T(X))$ of the optimally temperature-scaled model g_T for any $g \in \mathcal{S}$ satisfies:

$$\mathbb{E}_{X \sim \pi_X} [d_{\text{KL}}(\pi(Y \mid X), \hat{\pi}_T(Y \mid X))] \geq \Theta(\log k) \quad (4.1)$$

In other words, even with temperature scaling every $g \in \mathcal{S}$ is asymptotically no better than random.

Proof. We begin by first verifying that the set \mathcal{S} is large with high probability. Firstly, there are uncountably many strong ERM interpolators g , since the interpolator constraint is only on the finitely many points in \mathcal{X} (so behavior is unconstrained elsewhere on the input space), and with probability 1 these points do not coincide.

In order to show uniform $k/(2N)$ -confidence over each overlapping region, let us focus on a single class $y < k$ with $\tau(y) = 1$ (i.e. the class y is odd-numbered). In this case, the overlapping region is $[\beta_y + 1, \beta_y + 2]$ (see Definition 4.1). By a Chernoff bound, there are $\Theta(N/k)$ class y points in this region with probability $1 - \exp(-\Omega(N/k))$.

Now conditioning on each class y point x in the region, the probability that a class $y+1$ point falls in a $k/(2N)$ -neighborhood of x is $1/(2N)$ (since the class-conditional density of the class $y+1$ points

is uniform over $[\beta_y + 1, \beta_y + 3]$, and the class prior is uniform over $[k]$). Thus, by a union bound the probability that x has no class $y + 1$ neighbors is at least $1/2$. Now by another Chernoff bound, there are $\Theta(N/k)$ class y points with no $k/(2N)$ -neighborhood neighbors with probability at least $1 - \exp(-\Omega(N/k))$. Repeating this logic for each overlapping region (conditioning appropriately) and taking a union bound shows that the set \mathcal{S} is large with probability $1 - k \exp(-\Omega(N/k))$.

With uniform $k/(2N)$ -confidence in hand, our approach is straightforward: we will lower bound the expected KL divergence by considering just the divergence over the regions consisting of the unions of the confidence neighborhoods, over which temperature scaling can at best bring the softmax outputs to uniform over k ($1/k$). However, the ground truth conditional distribution over the confidence neighborhoods is uniform over only two classes (since the neighborhoods are in a region of overlap between two classes).

As before, for simplicity we will focus on a single class since the argument that follows can be iterated for each subsequent class. To keep notation brief, let us define:

$$H_\pi(\hat{\pi} \mathbb{1}_A) = \mathbb{E}_{\pi(Y|X)}[-\mathbb{1}_A \log \hat{\pi}(Y|X)] \quad (\text{A.1})$$

In other words, the cross-entropy restricted to a region A . Now consider a class $1 < y < k$ with $\tau(y) = 0$ (even parity); over its support $[\beta_y, \beta_y + 2]$ we observe that:

$$\begin{aligned} H_\pi(\pi \mathbb{1}_{[\beta_y, \beta_y + 2]}) &= -\frac{1}{2k} \int_{\beta_y}^{\beta_y + 2} \sum_{y \in [k]} \pi(Y = y | X = x) \log \pi(Y = y | X = x) dx \\ &= \frac{\log 2}{k} \end{aligned} \quad (\text{A.2})$$

So the entropy over the support of class y of the ground truth conditional distribution is a constant divided by k . We will now show that the entropy over the same region for the temperature-scaled predictive distribution $\hat{\pi}_T(Y|X)$ is lower bounded by $\Theta(\log(k)/k)$.

To do so, we will constrain our attention as mentioned earlier to the entropy over just the regions specified by $k/(2N)$ -confidence. Let U denote the union of all of the $k/(2N)$ -confidence neighborhoods around class $y - 1$ points in the region $[\beta_y, \beta_y + 1]$. Note that we are focusing on the neighborhoods around class $y - 1$ points (this corresponds to the odd-numbered class in our discussion above regarding uniform confidence), because in these neighborhoods the class y softmax output will be extremely small (due to the interpolation property applied to g on the class $y - 1$ points). We have that:

$$H_\pi(\hat{\pi}_T \mathbb{1}_{[\beta_y, \beta_y + 2]}) \geq -\frac{1}{2k} \min_{T > 0} \int_U \frac{1}{2} \log \phi^y(g(x)/T) dx \quad (\text{A.3})$$

Now we can lower bound the integrand in Equation (A.3) at each point $(x_i, y - 1) \in \mathcal{X}$ with $x_i \in U$ as:

$$\begin{aligned} -\log \phi^y(g(x_i)/T) &= -\log \frac{\exp(g^y(x_i)/T)}{\exp(g^{(y-1)}(x_i/T)) + \sum_{s \neq (y-1)} \exp(g^s(x_i)/T)} \\ &\geq -\log \frac{\exp(g^y(x_i)/T)}{\exp(g^{(y-1)}(x_i/T)) + (k-1) \exp((g^y(x_i) - C_i)/T)} \end{aligned} \quad (\text{A.4})$$

Where C_i above is from the ERM interpolation property of g . Applying uniform $k/(2N)$ -confidence we can translate the bound in Equation (A.4) to all $x \in U$ at the cost of introducing a $O(k/(2N))$ correction to $g^{(y-1)}(x_i/T)$ and a $O(1/k)$ correction to $\pi_X(U)$. Both of these error terms will be asymptotically irrelevant in our calculation. Letting \mathcal{X}_U denote all points $x_i \in U$ with $(x_i, y - 1) \in \mathcal{X}$ and recalling that $\mu_1(U)$ denotes the 1-dimensional Lebesgue measure of the set U , we then obtain:

$$\begin{aligned} H_\pi(\hat{\pi}_T \mathbb{1}_{[\beta_y, \beta_y + 2]}) &\geq \\ &\Theta \left(-\frac{\mu_1(U)}{k} \max_{x_i \in \mathcal{X}_U} \log \frac{\exp(g^y(x_i)/T)}{\exp(g^{(y-1)}(x_i/T)) + (k-1) \exp((g^y(x_i) - C_i)/T)} \right) \end{aligned} \quad (\text{A.5})$$

Now we consider two cases; $T < 1$ and $T \geq 1$. In the former case, since $\exp(g^{(y-1)}(x_i)) \geq k \exp(g^y(x_i))$, we have that the term inside the log is bounded above by $1/k$. In the latter case, since C_i is a constant, the term inside the log is also bounded above by $1/k$. Thus we get:

$$H_\pi(\hat{\pi}_T \mathbb{1}_{[\beta_y, \beta_y+2]}) \geq \Theta\left(\frac{\mu(U) \log k}{k}\right) \quad (\text{A.6})$$

Finally, we observe that U consists of the union of $\Theta(N/k)$ neighborhoods of size $\Theta(k/N)$, so $\mu(U) = \Theta(1)$. Iterating this argument over each of the $\lfloor k/2 \rfloor$ overlapping regions, we obtain the desired result. \square

As mentioned, the proof of the more general result follows the proof of Proposition 4.2 extremely closely, and we thus recommend reading the above proof before proceeding to this one (as we skip some details).

Theorem 4.5. Let \mathcal{X} consist of N i.i.d. draws from any distribution π satisfying Definition 4.4, and let $r \in \mathbb{R}$ be such that the sphere with radius r in \mathbb{R}^d has volume $k/(MN)$. Then the result of Proposition 4.2 still holds for the set \mathcal{S}_d of ERM interpolators for \mathcal{X} which are uniformly r -confident over each overlapping region in $\text{supp}(\pi_X)$.

Proof. As in the proof of Proposition 4.2, there are uncountably many ERM interpolators for \mathcal{X} . Now for showing that there is a subset of such interpolators satisfying uniform r -confidence over overlapping regions with high probability, let us consider a class y whose support overlaps with the supports of other classes $s_1(y), \dots, s_m(y)$ (as defined in Definition 4.4).

Let $A \subset \text{supp}(\pi_y)$ denote the overlap between the support of y and an arbitrary one of the aforementioned classes $s_i(y)$. As before, by a Chernoff bound, there are $\Theta(N/k)$ class y points falling in A with probability at least $1 - \exp(-\Omega(N/k))$.

Conditioning on each class y point x in A , the probability that a point from classes $s_1(y), \dots, s_m(y)$ falls in an r -neighborhood of x is $\alpha m/(MN)$ for some constant $\alpha < 1$ (since $\pi_X(A) \in [\Theta(1), 1 - \Theta(1)]$). As before, this implies by a union bound and another Chernoff bound that there are $\Theta(N/k)$ class y points with no r -neighborhood neighbors with probability at least $1 - \exp(-\Omega(N/k))$. Repeating this logic and taking another union bound, it follows that the set \mathcal{S} is large with probability at least $1 - k \exp(-\Omega(N/k))$.

The rest of the proof carries over similarly from the proof of Proposition 4.2. Let y be any class with overlaps, as considered above. Similarly, let s be any class overlapping with y whose region of overlap we denote as A , once again as above. Defining $H_\pi(\cdot)$ as in Equation (A.1), we see that:

$$H_\pi(\pi \mathbb{1}_{\text{supp}(\pi_s)}) = \Theta\left(\frac{1}{k}\right) \quad (\text{A.7})$$

Now letting U denote the union of all r -neighborhoods around class y points in the overlapping region A , we also get:

$$H_\pi(\hat{\pi}_T \mathbb{1}_{\text{supp}(\pi_s)}) \geq -\Theta\left(\frac{1}{k} \min_{T>0} \int_U \log \phi^s(g(x)/T) dx\right) \quad (\text{A.8})$$

As in the proof of Proposition 4.2, we can lower bound the integrand in Equation (A.8) at each point $(x_i, y) \in \mathcal{X}$ with $x_i \in U$ as:

$$-\log \phi^s(g(x_i)/T) \geq -\log \frac{\exp(g^s(x_i)/T)}{\exp(g^y(x_i/T)) + (k-1) \exp((g^s(x_i) - C_i)/T)} \quad (\text{A.9})$$

Once again letting \mathcal{X}_U denote all points $x_i \in U$ with $(x_i, y) \in \mathcal{X}$, we obtain from uniform r -confidence:

$$H_\pi(\hat{\pi}_T \mathbb{1}_{\pi_s}) \geq \Theta\left(-\frac{\mu_d(U)}{k} \max_{x_i \in \mathcal{X}_U} \log \frac{\exp(g^s(x_i)/T)}{\exp(g^y(x_i/T)) + (k-1) \exp((g^s(x_i) - C_i)/T)}\right) \quad (\text{A.10})$$

Which, by identical logic to the proof of Proposition 4.2, gives:

$$H_\pi(\hat{\pi}_T \mathbb{1}_{\pi_s}) \geq \Theta\left(\frac{\mu_d(U) \log k}{k}\right) \quad (\text{A.11})$$

Observing again that $\mu_d(U) = \Theta(1)$ and applying this logic to all $\Theta(k)$ overlapping regions in $\text{supp}(\pi_X)$, we obtain the desired result. \square

A.2 Mixup Optimality Lemma and Proofs of Proposition 4.3 and Theorem 4.6

First, we provide a proper definition of the mixing set $\mathcal{M}_d(\mathcal{X})$, which was intuitively described in Section 3.3 of the main paper.

Definition A.1. Given a dataset \mathcal{X} , we define:

$$\begin{aligned} \mathcal{M}_d(\mathcal{X}) = \left\{ \sigma \in [N]^{d+1} : x_{\sigma_i} - x_{\sigma_{d+1}} \neq 0 \quad \forall i \in [d] \right. \\ \text{and} \quad \frac{\langle x_{\sigma_i} - x_{\sigma_{d+1}}, x_{\sigma_j} - x_{\sigma_{d+1}} \rangle}{\|x_{\sigma_i} - x_{\sigma_{d+1}}\| \|x_{\sigma_j} - x_{\sigma_{d+1}}\|} \leq \frac{1}{2d} \quad \forall i, j \in [d], i \neq j \\ \left. \text{and} \quad \|x_{\sigma_i} - x_{\sigma_j}\| \leq C(\mathcal{X}) \quad \forall i, j \in [d+1] \right\} \end{aligned}$$

Where $C(\mathcal{X})$ is a possibly data-dependent constant.

We recall that the definition of $\mathcal{X}_{\text{mix},d}$ is all z such that $z = \sum_{j \in [d+1]} \lambda_j x_{\sigma_j}$ for some $\lambda \in \text{supp}(\mathcal{D}_{\lambda,d})$ and $\sigma \in \mathcal{M}_d(\mathcal{X})$. Now we prove a formal version of Lemma 3.3, which we will rely on in the proofs of Proposition 4.3 and Theorem 4.6.

Lemma A.2. Let f_λ denote the density of $\mathcal{D}_{\lambda,d}$ and define:

$$L_\sigma = \begin{bmatrix} x_{\sigma_1} - x_{\sigma_{d+1}} & x_{\sigma_2} - x_{\sigma_{d+1}} & \dots & x_{\sigma_d} - x_{\sigma_{d+1}} \end{bmatrix} \quad (\text{A.12})$$

$$\Lambda_\sigma(z) = \begin{bmatrix} L_\sigma^{-1}(z - x_{\sigma_{d+1}}) & 1 - \sum_{j \in [d]} L_\sigma^{-1}(z - x_{\sigma_{d+1}})_j \end{bmatrix} \quad (\text{A.13})$$

$$\alpha_y(z) = \sum_{\sigma \in \mathcal{M}_d(\mathcal{X})} \mathbb{1}_{z \in \text{conv}(\{x_{\sigma_i}\}_{i=1}^{d+1})} |\det(L_\sigma^{-1})| f_\lambda(\Lambda_\sigma(z)) \sum_{j: y_{\sigma_j} = y} \Lambda_\sigma(z)_j \quad (\text{A.14})$$

Then any $g^* \in \arg\inf_g J_{\text{mix},d}(g, \mathcal{X}, \mathcal{D}_{\lambda,d})$ satisfies $\phi^y(g^*(z)) = \alpha_y(z) / \sum_{s \in [k]} \alpha_s(z)$ for almost every $z \in \mathcal{X}_{\text{mix},d}$.

Proof. First, writing out the expectation in Equation (3.8), we have:

$$J_{\text{mix},d}(g, \mathcal{X}, \mathcal{D}_{\lambda,d}) = -\frac{1}{|\mathcal{M}_d(\mathcal{X})|} \sum_{\sigma \in \mathcal{M}_d(\mathcal{X})} \int_{\Delta^d} \sum_{i \in [d+1]} \lambda_i \log \phi^{y_{\sigma_i}} \left(g \left(\sum_{j \in [d+1]} \lambda_j x_{\sigma_j} \right) \right) f(\lambda) d\lambda \quad (\text{A.15})$$

Now we make the substitution $z = \sum_{j \in [d+1]} \lambda_j x_{\sigma_j}$. By the definition of $\mathcal{M}_d(\mathcal{X})$, the transformation L_σ in Equation (A.12) is invertible, so $\Lambda_\sigma(z)$ from Equation (A.13) is well-defined. Now applying Fubini's Theorem, we may write:

$$\ell(\sigma, z) = -|\det(L_\sigma^{-1})| f_\lambda(\Lambda_\sigma(z)) \sum_{j \in [d+1]} \Lambda_\sigma(z)_j \log \phi^{y_{\sigma_j}}(g(z)) \quad (\text{A.16})$$

$$J_{\text{mix},d}(g, \mathcal{X}, \mathcal{D}_{\lambda,d}) = \frac{1}{|\mathcal{M}_d(\mathcal{X})|} \int_{\mathcal{X}_{\text{mix},d}} \sum_{\sigma \in \mathcal{M}_d(\mathcal{X})} \mathbb{1}_{z \in \text{conv}(\{x_{\sigma_i}\}_{i=1}^{d+1})} \ell(\sigma, z) dz \quad (\text{A.17})$$

We observe that $\sum_{\sigma \in \mathcal{M}_d(\mathcal{X})} \mathbb{1}_{z \in \text{conv}(\{x_{\sigma_i}\}_{i=1}^{d+1})} \ell(\sigma, z)$ is strictly convex as a function of $\phi(g(z))$. Now we can optimize the aforementioned term as a function of $\phi(g(z))$ under the constraint that $\sum_{y \in [k]} \phi^y(g(z)) = 1$. This is straightforward to do with Lagrange multipliers, and the solution is of the form $\phi^y(g(z)) = \alpha_y(z) / \sum_{s \in [k]} \alpha_s(z)$ where $\alpha_y(z)$ is defined as in Equation (A.14), so the result follows. \square

With Lemma A.2, we can prove Proposition 4.3.

Proposition 4.3. Let \mathcal{X} be as in Proposition 4.2 and $p(k)$ denote a polynomial in k of degree at least one. Then taking $\mathcal{D}_{\lambda,1}$ to be uniform, every 1-Mixup interpolator g for \mathcal{X} with the property that $\phi^y(g(x)) \leq 1 - \Omega(1/p(k))$ for every $x \in \text{supp}(\pi_X) \setminus \mathcal{X}_{\text{mix},1}$ and $y \in [k]$ satisfies with probability at least $1 - k^2 \exp(-\Omega(N/k^2))$:

$$\mathbb{E}_{X \sim \pi_X} [d_{\text{KL}}(\pi(Y | X), \hat{\pi}(Y | X))] \leq \Theta(1) \quad (4.2)$$

Proof. We first partition $\text{supp}(\pi_X)$ into subregions each of which have measure $\Theta(1/k)$, so that there are $\Theta(k^2)$ total subregions. By a Chernoff bound, there are $\Theta(N/k^2)$ points in each of these subregions with probability at least $1 - \exp(-\Omega(N/k^2))$. Thus, by a union bound, the probability that every subregion contains $\Theta(N/k^2)$ points is at least $1 - k^2 \exp(-\Omega(N/k^2))$. Consequently, with the same probability, $\pi_X(\text{supp}(\pi_X) \setminus \mathcal{X}_{\text{mix},d}) = O(1/k)$. To see this, observe that for z to be in $\mathcal{X}_{\text{mix},d}$, we need only have one point to the left of z and one point to the right of z , both within a constant distance of one another (note that the other conditions in $\mathcal{M}_d(\mathcal{X})$ are vacuously satisfied since we are in dimension 1). By our high probability arguments, there is at most some $O(1/k)$ Lebesgue measure region in each pair of overlapping class intervals with no points in \mathcal{X} , from which it follows that $\pi_X(\text{supp}(\pi_X) \setminus \mathcal{X}_{\text{mix},d}) = O(1/k)$.

Now for $y \in [k]$, consider $z \in \text{supp}(\pi_y) \cap \mathcal{X}_{\text{mix},d}$. We will show that every 1-Mixup interpolator g for \mathcal{X} with $\mathcal{D}_{\lambda,1}$ being uniform satisfies $\phi^y(g(z)) \in [\Theta(1), 1]$ when z falls only in the support of y and $\phi^y(g(z)) \in [\Theta(1), 1 - \Theta(1)]$ in the overlapping region, which will be sufficient for showing the desired result.

Suppose without loss of generality that $\tau(y) = 1$ and that $y < k$ (i.e. y is an odd-numbered class), and consider first $z \in [\beta_y, \beta_y + 1] \cap \mathcal{X}_{\text{mix},d}$ (the non-overlapping part of $\text{supp}(\pi_y)$). Clearly z can only be obtained from $\sigma \in \mathcal{M}_d(\mathcal{X})$ with $y_{\sigma_1} = y$ or $y_{\sigma_2} = y$, since the other class supports are spaced k away and $z \in \text{supp}(\pi_y) \setminus \text{supp}(\pi_{y+1})$. This implies that for $g^* \in \text{arginf}_g J_{\text{mix},1}(g, \mathcal{X}, \mathcal{D}_{\lambda,1})$, we have $\alpha_s(z) = 0$ for $s \neq y, y+1$ (where α_y is as in Equation (A.14)). Now we consider two sub-cases: $z \in [\beta_y, \beta_y + 1/2]$ and $z \in [\beta_y + 1/2, \beta_y + 1]$.

In the first sub-case, if $y_{\sigma_j} = y$ then $\lambda_j \geq 1/2$ since $z = \lambda_1 x_{\sigma_1} + (1 - \lambda_1) x_{\sigma_2}$ must necessarily fall closer to whichever class y point produced it, which implies that $\alpha_y(z) \geq \alpha_{y+1}(z)$. For the latter sub-case, we recall that by our high probability arguments there are $\Theta(N/k)$ class y points in $[\beta_y, \beta_y + 1/2]$, which implies there are $\Theta(N^2/k^2)$ choices of $\sigma \in \mathcal{M}_d(\mathcal{X})$ which can produce $z \in [\beta_y + 1/2, \beta_y + 1]$ with a constant weight associated with class y . Since there are $O(N^2/k^2)$ total choices of $\sigma \in \mathcal{M}_d(\mathcal{X})$ that can produce $z \in [\beta_y + 1/2, \beta_y + 1]$, we get that $\alpha_y(z) = \Omega(\alpha_{y+1}(z))$ in this case. Now from Definition 3.4, it immediately follows that every 1-Mixup interpolator g satisfies $\phi^y(g(z)) \in [\Theta(1), 1]$ for $z \in [\beta_y, \beta_y + 1]$.

Let us now consider $z \in [\beta_y + 1, \beta_y + 2] \cap \mathcal{X}_{\text{mix},d}$ (the overlapping part of $\text{supp}(\pi_y)$). We can apply similar logic to that used in handling the sub-case of $z \in [\beta_y + 1/2, \beta_y + 1]$ considered above; namely, for every $z \in [\beta_y + 1, \beta_y + 2]$, there are $\Theta(N^2/k^2)$ choices of $\sigma \in \mathcal{M}_d(\mathcal{X})$ which can produce z with a constant weight associated with class y (mixing with points in $[\beta_y, \beta_y + 1]$), and so as before we get that $\alpha_y(z) = \Omega(\alpha_{y+1}(z))$. However, there are also $\Theta(N^2/k^2)$ choices of $\sigma \in \mathcal{M}_d(\mathcal{X})$ which can produce z with a constant weight associated with class $y+1$ (mixing with points in $[\beta_y + 2, \beta_y + 3]$), so we also get $\alpha_{y+1}(z) = \Omega(\alpha_y(z))$. Thus, it follows that g satisfies $\phi^y(g(z)) \in [\Theta(1), 1 - \Theta(1)]$ for $z \in [\beta_y + 1, \beta_y + 2] \cap \mathcal{X}_{\text{mix},d}$.

Based on the above, we see that $H_\pi(\hat{\pi} \mathbb{1}_{\mathcal{X}_{\text{mix},1}}) = \Theta(1)$ (where we recall that H_π is defined as in Equation (A.1)). Furthermore, since $\phi^y(g(x)) \leq 1 - \Omega(1/\text{poly}(k))$ on $\text{supp}(\pi_X) \setminus \mathcal{X}_{\text{mix},1}$, we have $H_\pi(\hat{\pi} \mathbb{1}_{\text{supp}(\pi_X) \setminus \mathcal{X}_{\text{mix},1}}) = O(\log(k)/k)$, from which the overall result follows. \square

Before proving Theorem 4.6, we need to formally state the necessary assumptions alluded to in the main text. Once again, these generalize the core facets of the simple data distribution from Definition 4.1.

Assumption A.3. In what follows, \mathcal{X} is understood to be N i.i.d. draws from π and $\mathcal{X}_{\text{mix},d}$ is obtained from \mathcal{X} as defined above and in Section 3.3. With this in mind, we restrict the class of distributions π from Definition 4.4 such that:

1. (Non-overlapping classes are separated) For $y, s \in [k]$, if $\pi_X(\text{supp}(\pi_y) \cap \text{supp}(\pi_s)) = 0$, then $d(\text{supp}(\pi_y), \text{supp}(\pi_s)) = \omega(1)$. Additionally, $\text{supp}(\pi_y) = \Theta(1)$ for all $y \in [k]$.
2. (Mixed points cover support) With probability at least $1 - k^2 \exp(-\Omega(N/k^2))$, $\pi_X(\text{supp}(\pi_X) \setminus \mathcal{X}_{\text{mix},d}) = O(1/k)$.
3. (Mixed points are balanced across overlapping classes) Let us define for $y \in [k]$ and $z \in \mathbb{R}^d$:

$$\mathcal{M}_d^y(\mathcal{X}, z) = \left\{ \sigma \in \mathcal{M}_d(\mathcal{X}) : \exists \lambda \in \text{supp}(\mathcal{D}_{\lambda,d}) \mid z = \sum_{j \in [d+1]} \lambda_j x_{\sigma_j} \text{ and } \sum_{j: y_{\sigma_j} = y} \lambda_j = \Theta(1) \right\} \quad (\text{A.18})$$

Then with probability at least $1 - k^2 \exp(-\Omega(N/k^2))$, for every $y \in [k]$ and $z \in \mathcal{X}_{\text{mix},d} \cap \text{supp}(\pi_y)$ we have that $|\mathcal{M}_d^y(\mathcal{X}, z)| = \Omega(N^d/k^d)$ or we have for every $\sigma \in \mathcal{M}_d(\mathcal{X})$ such that $z = \sum_{j \in [d+1]} \lambda_j x_{\sigma_j}$ with $\lambda \in \text{supp}(\mathcal{D}_{\lambda,d})$:

$$\sum_{j: y_{\sigma_j} = y} \lambda_j \geq \sum_{i: y_{\sigma_i} \neq y} \lambda_i \quad (\text{A.19})$$

The third part of Assumption A.3 appears complicated, but it just generalizes one of the key ideas in the proof of Proposition 4.2: either our mixed points always fall closer to one class (i.e. they are far away from the overlapping region), or there are a lot of possible mixings that can produce the mixed point. Ideally we would have structured Assumption A.3 to be purely in terms of the shape of π (as discussed in Section 5 in the main paper) and not in terms of the high probability behavior of the mixed points $\mathcal{X}_{\text{mix},d}$, but various edge cases in high dimensions led us to structuring the assumption this way.

With this assumption, it is straightforward to prove the generalization of Proposition 4.2.

Theorem 4.6. Let \mathcal{X} consist of N i.i.d. draws from any distribution π satisfying Definition 4.4 and Assumption A.3, and let $p(k)$ be as in Proposition 4.3. Then the result of Proposition 4.3 still holds when considering d -Mixup interpolators g for \mathcal{X} where the mixing distribution $\mathcal{D}_{\lambda,d}$ is uniform over the d -dimensional probability simplex.

Proof. Assumption A.3 allows us to largely lift the proof of Proposition 4.2 to higher dimensions. Indeed, from the second part of Assumption A.3 we already begin with the fact that $\pi_X(\text{supp}(\pi_X) \setminus \mathcal{X}_{\text{mix},d}) = O(1/k)$ with probability at least $1 - k^2 \exp(-\Omega(N/k^2))$.

Now as before, for $y \in [k]$, consider $z \in \text{supp}(\pi_y) \cap \mathcal{X}_{\text{mix},d}$. By the first part of Assumption A.3 and Definition A.1, z can only be obtained by mixing points from class y and/or its overlapping neighbors $s_1(y), \dots, s_m(y)$.

If $z \notin \text{supp}(\pi_{s_i(y)})$ for every $s_i(y)$ (i.e. it is not in the overlapping region), then by the third part of Assumption A.3 it immediately follows that $\phi^y(g(z)) \in [\Theta(1), 1]$. On the other hand, if $z = \sum_{j \in [d+1]} \lambda_j x_{\sigma_j} \in \text{supp}(\pi_{s_i(y)})$ for some $s_i(y)$, then we cannot simultaneously satisfy:

$$\sum_{j: y_{\sigma_j} = y} \lambda_j \geq \sum_{r: y_{\sigma_r} \neq y} \lambda_r \quad \text{and} \quad \sum_{j: y_{\sigma_j} = s_i(y)} \lambda_j \geq \sum_{r: y_{\sigma_r} \neq y} \lambda_r \quad (\text{A.20})$$

This implies that the other condition in the third part of Assumption A.3 is satisfied for both y and $s_i(y)$; i.e. $|\mathcal{M}_d^y(\mathcal{X}, z)| = \Omega(N^d/k^d)$ (see Equation (A.18)). Since there are $O(N^d/k^d)$

$\sigma \in \mathcal{M}_d(\mathcal{X})$ that could have produced z with probability at least $1 - k \exp(-\Omega(N/k))$ (by the usual Chernoff bound), this implies that $\phi^y(g(z)) \in [\Theta(1), 1 - \Theta(1)]$. As in the final part of the proof of Proposition 4.3, from this we get $H_\pi(\hat{\pi} \mathbb{1}_{\mathcal{X}_{\text{mix},d}}) = \Theta(1)$ and we are done from the fact that $\phi^y(g(x)) \leq 1 - \Omega(1/\text{poly}(k))$ on $\text{supp}(\pi_X) \setminus \mathcal{X}_{\text{mix},d}$. \square

B Additional Experiments

All experiments described in this section follow the same experimental setup as Section 2.1, unless otherwise stated.

B.1 Logit Plots

Here we include the logit equivalents of Figures 2 and 3; i.e. instead of plotting the mean original class probability, we plot the mean original class logit. The results are shown in Figures 5 and 6.

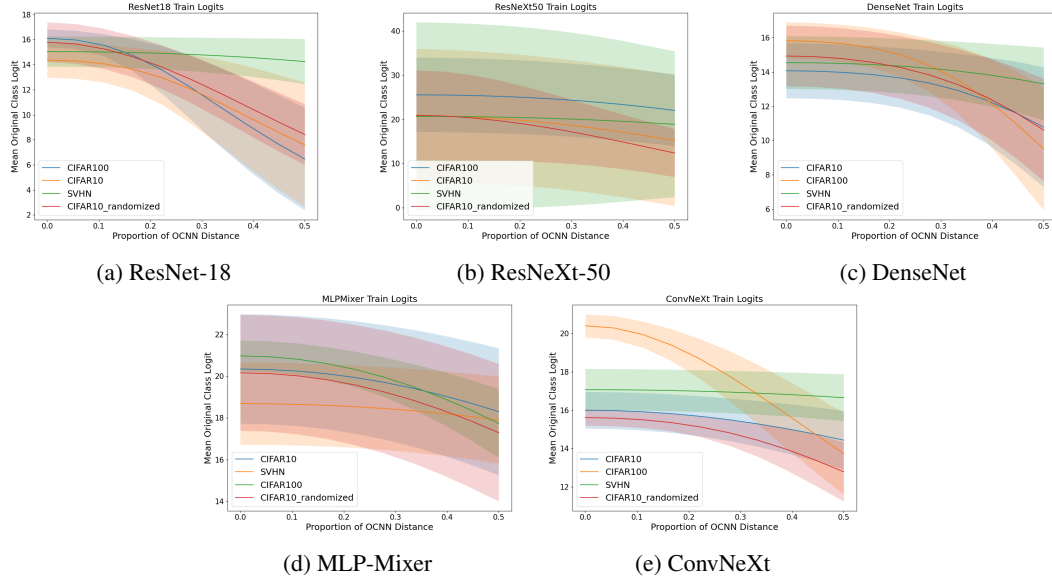


Figure 5: Mean original class logits for different models trained with empirical risk minimization (ERM). The shaded regions around each curve represent one standard deviation.

We make two main observations regarding Figures 5 and 6: the original class logit has significantly more variability than the softmax output, and the Mixup logits are significantly smaller than the ERM logits. The latter phenomenon is consistent with our discussion of neighborhood constraints in Section 3.3; intuitively, it should be easier to achieve the Mixup-optimal behavior of linearly interpolating probabilities between data points with smaller logits.

For the former observation, the logit variability is negligible when considering the *gap* between the original class logit and the second largest logit (the second most likely class), which is what leads to such low variability in the softmax outputs. The logit gap plots for ERM and Mixup are shown in Figures 7 and Figures 8.

From comparing the original class logit plots to the original class logit gap plots for empirical risk minimization, we see that in essentially all cases the plots show very similar values; in other words, the second largest logit is near zero, which is what motivated Definition 3.1.

B.2 Impact of Training Horizon on Uniform Confidence

To understand the effect of training horizon on uniform confidence, we repeat the experiments of Section 2 but consider stopping training at 10, 50, and 250 epochs instead of the 500 epochs of training used for the experiments in the main paper. Both for simplicity and for compute reasons,

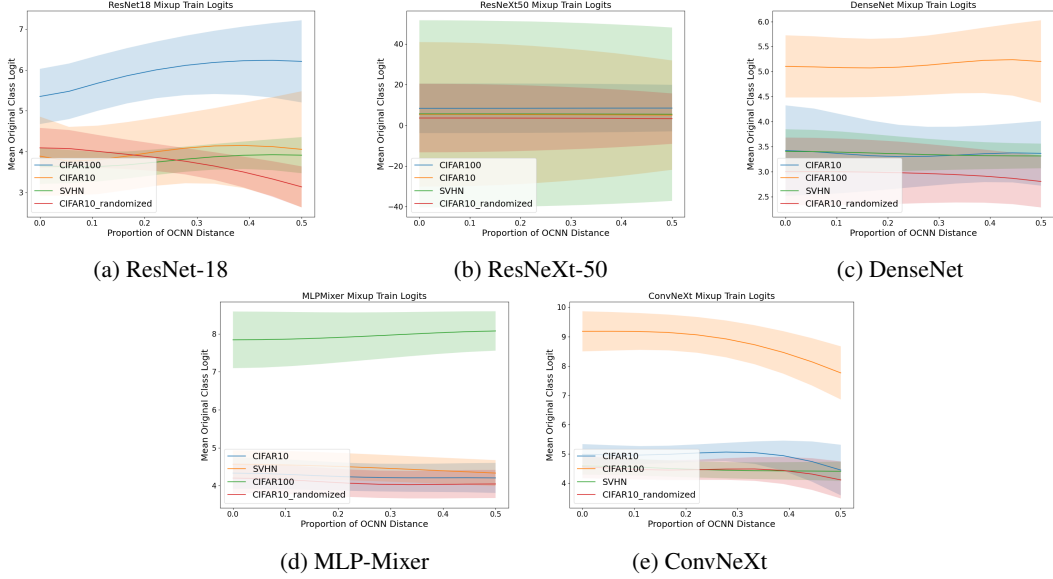


Figure 6: Mean original class logits for Mixup (uniform mixing distribution).

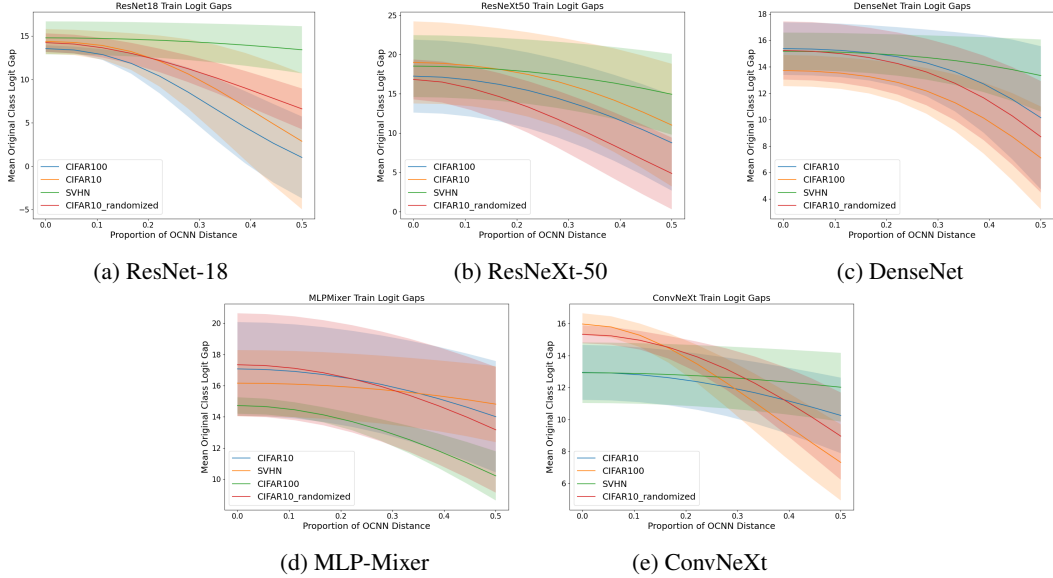


Figure 7: Mean original class logit gap with second largest logit for ERM.

we repeat the experiments on just the single dataset CIFAR-10, since all of our other experimental results have been largely consistent across datasets. The results are shown in Figure 9.

From Figure 9, we see in fact that several models exhibit uniform-confidence-like behavior even with only 50 epochs of training (ResNet-18, MLP-Mixer, and ConvNeXt). At 250 epochs of training, the results appear near-identical to the ones shown in the main paper. Importantly, for the curves which have very little variance at 0.0-0.2 OCNN distance, we observe that the corresponding models have reached the interpolation regime; i.e. the have achieved zero training error. As emphasized in the main text, this appears to empirically be sufficient for uniform confidence.

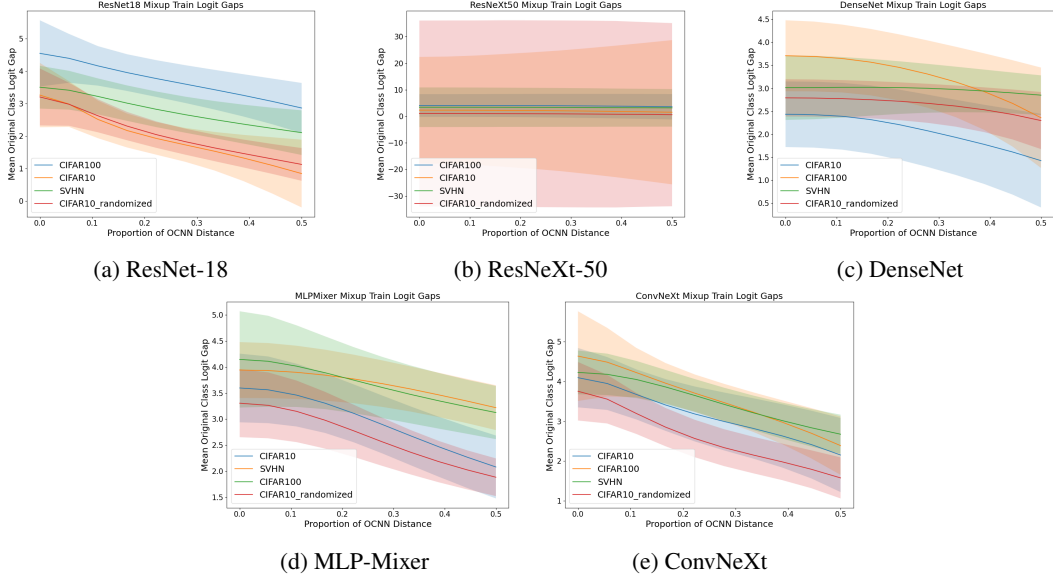


Figure 8: Mean original class logit gap with second largest logit for Mixup.

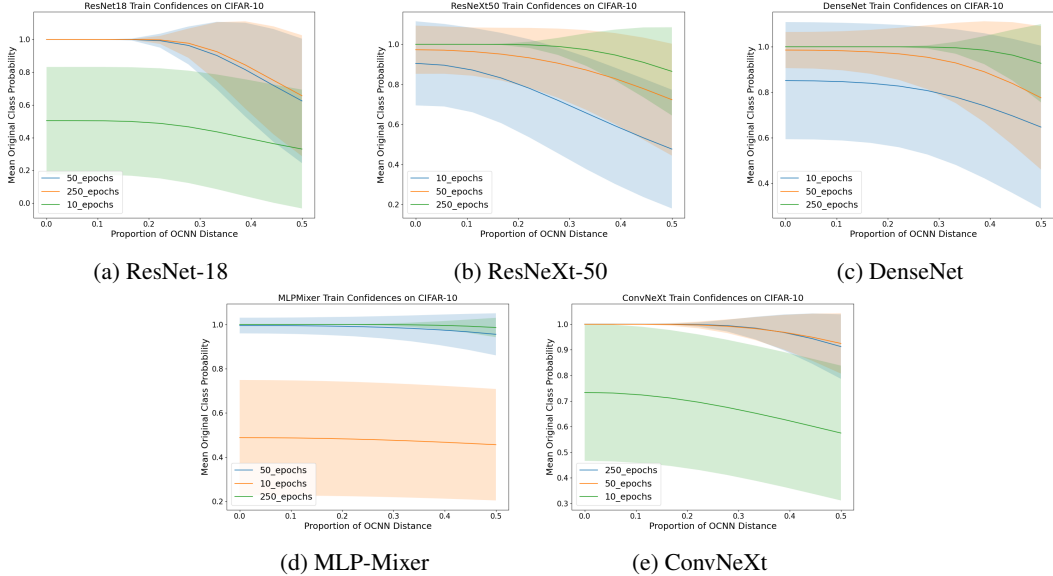


Figure 9: Mean original class softmax output for different training horizons on CIFAR-10 for models trained with empirical risk minimization.

B.3 Confidence on Test Data

Similar to how we downsampled each training dataset in Section 2.1 to consist of 5000 data points, we also downsample each test dataset to consist of 1000 data points (once again, approximately 10% of the original data). The results of repeating the experiments of Section 2 (using the same trained models) on the held-out test data is shown in Figures 10 and 11.

We see from Figure 10 that, as one would guess, uniform confidence behavior in this case does not translate to the test data - this can be attributed to the fact that the trained models do not have perfect test performance, which inevitably leads to more variance and a mean softmax output that is not approximately 1. That being said, we find it interesting that even given the fact that we trained on a subsampled version of the original training data, model confidence is still in the 0.9-1.0 range for several model/dataset pairs on the held-out test data.

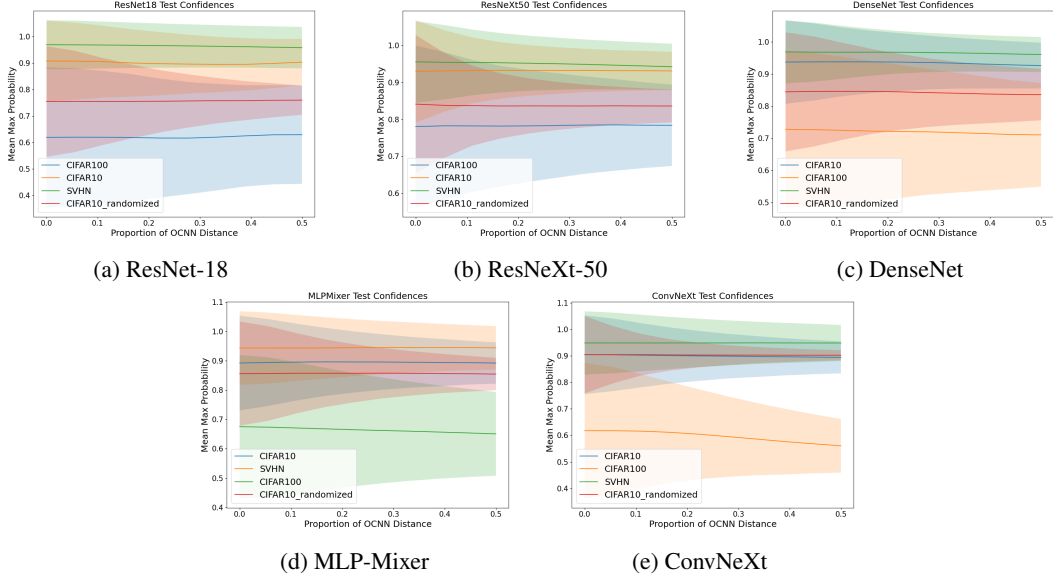


Figure 10: Mean original class softmax output on held-out test data for models trained with ERM.

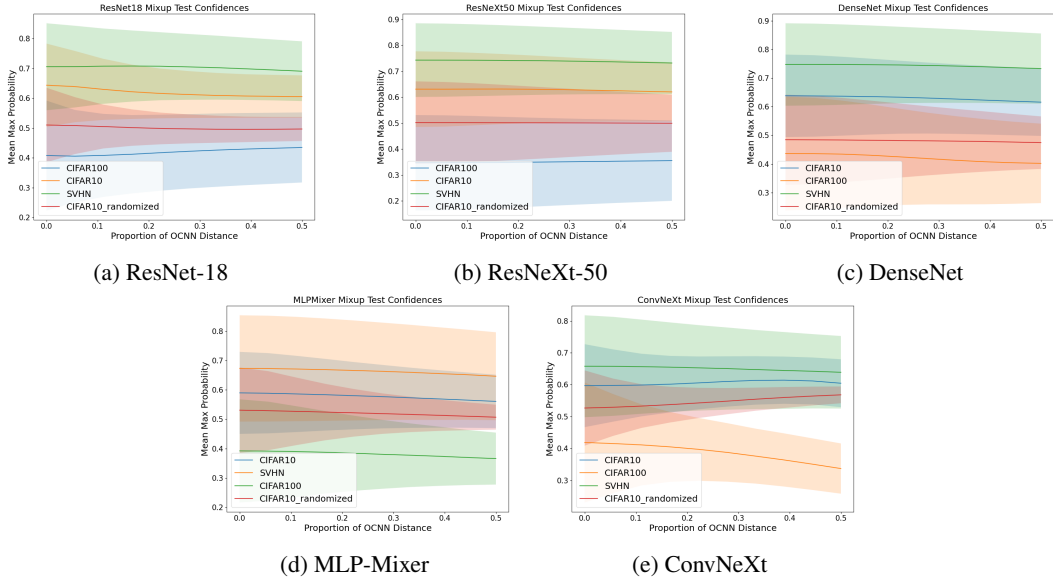


Figure 11: Mean original class softmax output on held-out test data for models trained with Mixup.

B.4 Full-Scale Data

In computing the OCNN distances in Section 2, we observed that the minimum OCNN distance across all datasets was approximately 10. With this knowledge, we can circumvent the quadratic cost associated with computing nearest neighbors and repeat the experiments of Section 2 *on the full datasets* by considering a fixed radius of 10 around each point. The results of doing so are shown in Figures 12 and 13.

As can be seen in Figure 12, uniform confidence largely persists even at full data scale. The curves with slightly larger (note the scale of the y-axis) standard deviation bands in Figure 12 correspond to models that did not achieve zero training error, and again we observe that reaching the interpolation regime appears to be important for uniform confidence. We point out that there is one anomalous result in Figure 12; namely, ConvNeXt failed to train (under our settings) on the randomized version

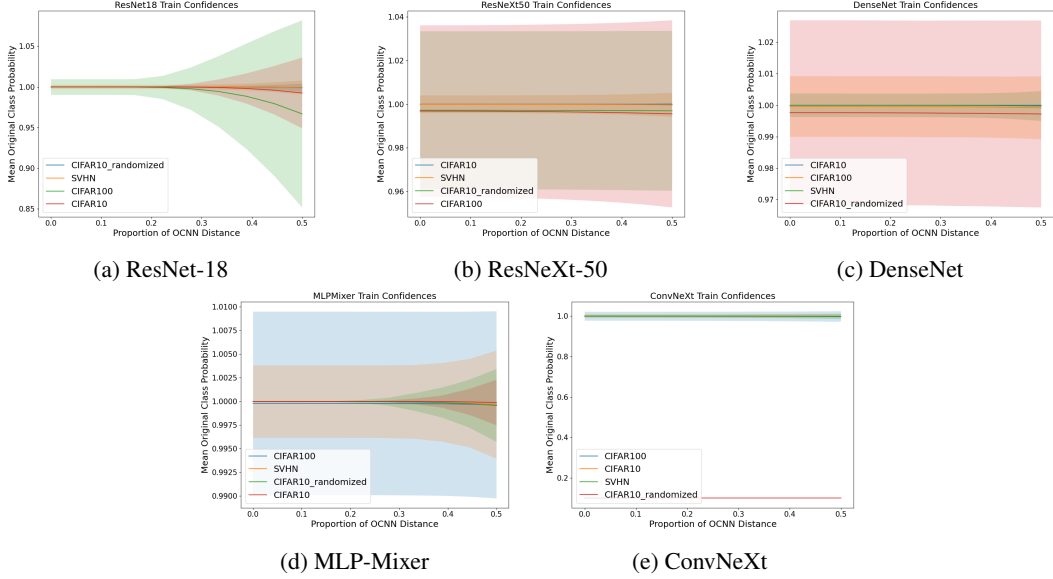


Figure 12: Mean original class softmax outputs for different models trained on full-scale datasets using empirical risk minimization.

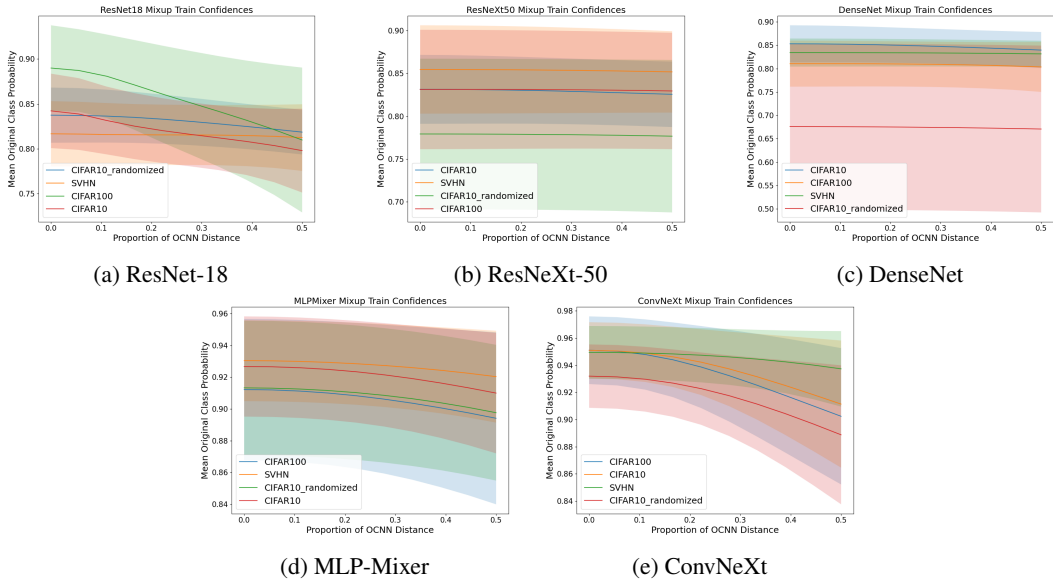


Figure 13: Mean original class softmax outputs for different models trained on full-scale datasets using Mixup.

of CIFAR-10. We do not investigate this further and expect that this could likely be fixed with different hyperparameters, as the model trained properly in the case of Mixup (Figure 13).